Bandlike Character of 4f Electrons in $CeRh_3$

E. Weschke, C. Laubschat, R. Ecker, A. Höhr, M. Domke, and G. Kaindl
Institut für Experimentalphysik, Freie Universität Berlin, Arnimallee 14, W-1000 Berlin 33, Germany

L. Severin and B. Johansson
Condensed Matter Theory Group, Physics Department, University of Uppsala, Box 530, S-75121 Uppsala, Sweden
(Received 21 January 1992)

The electronic structure of $CeRh_3$ was studied by photoemission and bremsstrahlung isochromate spectroscopy (BIS). An analysis of the spectra, taken at different temperatures, on the basis of the Anderson single-impurity model leads to considerable inconsistencies that mark the limits of applicability of the model. On the other hand, the BIS spectrum of $CeRh_3$ can be well described by the results of a local-density-approximation band-structure calculation. These findings confirm a bandlike character of the 4f states in strongly hybridized Ce systems.

PACS numbers: 71.28.+d, 73.20.At, 79.60.−i

For quite some time, the electronic structure of Ce systems has attracted a wide scope of experimental and theoretical efforts, but the nature of the 4f states —bandlike versus localized—remains controversial. While itinerant-electron models were proposed to explain ground-state properties, in particular the $\gamma \rightarrow \alpha$ phase transition of Ce metal [1–3], they seem to fail in describing the observed correlation effects in high-energy excitation spectra. On the other hand, the latter effects as well as ground-state properties have been consistently described within the Anderson model, which treats the 4f states as single impurities (SI) hybridized with the valence band [4–6], but neglects direct interactions between neighboring impurities. If these interactions become significant, a bandlike description of the 4f states can be more favorable [7], where the remaining correlation effects have to be introduced in an analogous way as in the case of Ni [8].

In this Letter, we present the results of high-energy spectroscopies for $CeRh_3$, which clearly suggest a description of the 4f states beyond the SI model in the case of this strongly hybridized Ce compound [9]. We find that the 4f photoemission (PE) spectra as well as the results of a high-resolution PE study of the Fermi-level region cannot be described consistently within the SI model in comparison to the temperature dependence of the 3d core-level PE spectra. An even stronger discrepancy is found for the bremsstrahlung isochromate spectrum (BIS) of $CeRh_3$, which—on the other hand—can be well described by the density of states from a local-density-approximation (LDA) band-structure calculation. These findings represent the first direct spectroscopic observation of 4f-band aspects in a rare-earth system.

The PE experiments were performed at the Berliner Elektronenspeicherring für Synchrotronstrahlung (BESSY). Valence-band spectra were taken at the high-resolution SX700/II beamline of the Freie Universität Berlin with a hemispherical Leybold EA-11 electron-energy analyzer. 3d core-level spectra were taken at the double-crystal monochromator (KMC) with a hemispherical VG CLAM-100 analyzer. BIS measurements were performed with a home-built spectrometer equipped with a spherically bent quartz-crystal monochromator ($h\nu$ = 1486.6 eV). Polycrystalline samples of $CeRh_3$ were prepared by arc melting in Ar atmosphere and characterized by x-ray diffraction. The sample surface was cleaned *in situ* (UHV of typically 10^{-10} mbars) by repeated scraping with a diamond file until no oxygen contamination could be detected (monitored by the O 2p and O 1s PE signals, respectively). For the PE measurements, the sample could be cooled to 20 K by a closed-cycle He refrigerator. The electronic-structure calculations were performed with the linear-muffin-tin-orbital method [10] including spin-orbit coupling at the variational step and employing the von Barth–Hedin exchange-correlation functional [11]. The one-electron density of states was calculated with the tetrahedron method [12], where eigenvalues are computed for a mesh of 135 **k** points in the irreducible part of the Brillouin zone.

We first investigated effects of temperature on 4f hybridization in $CeRh_3$. The results are shown in Fig. 1: (a) Ce 3d core-level PE spectra; (b) 4f PE spectra. The Ce 3d core-level PE spectra consist of three spin-orbit-split doublets (C,D,E) due to three different final states that are roughly characterized by $4f^2$ (C), $4f^1$ (D), and $4f^0$ (E) configurations [9]. Weakly hybridized γ-like systems show mainly doublet D, while α-like systems, like $CeRh_3$, exhibit considerable intensity in the doublets C and E reflecting strong 4f hybridization. Upon cooling of $CeRh_3$ to 20 K, an increase in the weights of doublets C and E occurs, visible, e.g., in the observed change of the intensity ratio of the two peaks marked by vertical arrows in Fig. 1(a). This weight increase corresponds to an increase in 4f hybridization at low temperatures.

The two subspectra in Fig. 1(a) represent the results of a detailed analysis as described in Ref. [13], which takes into account emission from the bulk and from the outer-

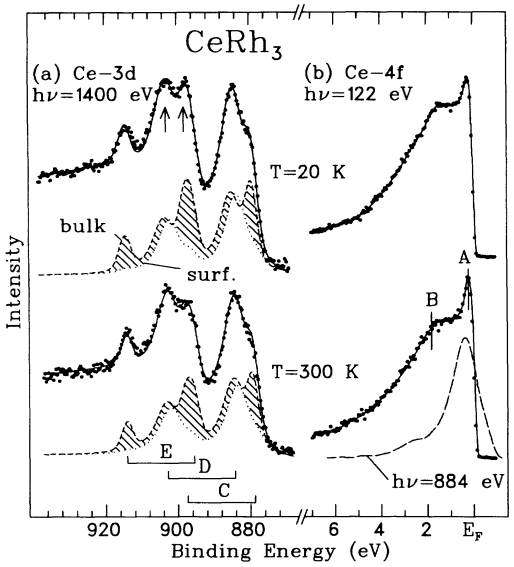

FIG. 1. PE spectra of $CeRh_3$ at $T=300$ K and $T=20$ K: (a) Ce $3d$ core-level spectra; (b) Ce $4f$ spectra taken in $4d \rightarrow 4f$ resonance ($h\nu=122$ eV) and corrected for non-$4f$ contributions. The long-dashed spectrum in (b) was taken in $3d \rightarrow 4f$ resonance ($h\nu=884$ eV). The dashed and dotted curves in (a) represent bulk and surface components. The total-system resolution (FWHM) was $\simeq 1.6$ eV in (a), while in (b) it was $\simeq 200$ meV (solid points) and $\simeq 0.7$ eV (long-dashed spectrum).

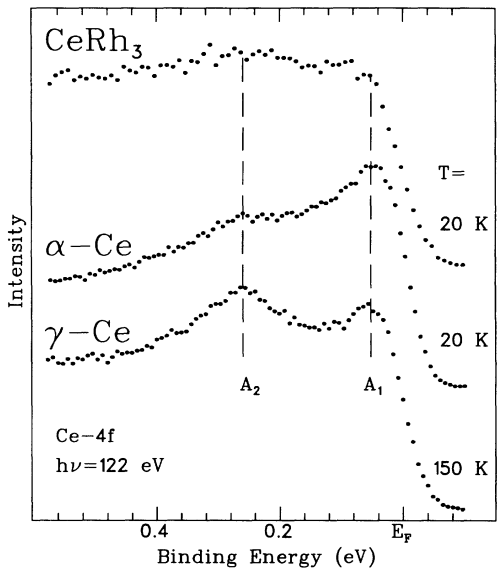

FIG. 2. $4f$-PE spectra of γ-Ce, α-Ce, and $CeRh_3$ taken in $4d \rightarrow 4f$ resonance; the total-system resolution was $\simeq 40$ meV (FWHM). The spectra have not been corrected for non-$4f$ contributions, since the latter are structureless and very weak in the region close to E_F.

most atomic surface layer and is based on the simplified SI model of Imer and Wouilloud [14]. For bulk $CeRh_3$ (hatched subspectra), the analysis results in an increase of $4f$ hybridization Δ at low temperatures: $\Delta^b=0.92 \pm 0.03$ eV at 300 K and $\Delta^b=1.57 \pm 0.03$ eV at 20 K, corresponding to $4f$ occupancies of $n_f^b=0.81 \pm 0.03$ at 300 K and $n_f^b=0.75 \pm 0.03$ at 20 K. The surface of $CeRh_3$ is found to be more γ-like, with $n_f^s=0.97 \pm 0.03$ at 300 K and $n_f^s=0.96 \pm 0.03$ at 20 K. These temperature changes are fully reversible and can be anticipated as a consequence of increasing internal pressure favoring the higher valency at low temperatures, similar to the situation in mixed-valent rare-earth systems [15].

The strong increase in bulk $4f$ hybridization responsible for the decrease in n_f at low temperatures should also be reflected in the $4f$ PE spectra displayed in Fig. 1(b). These spectra were taken in $4d \rightarrow 4f$ resonance at $h\nu=122$ eV, where residual non-$4f$ contributions were eliminated by subtracting properly normalized off-resonance spectra taken at $h\nu=112$ eV [5]. The resulting spectra are dominated by $4f$ emission and show the well-known splitting into two components A and B. Peak B is at a binding energy of $\simeq 2$ eV and corresponds to a $4f^0$ final state, while peak A is situated very close to E_F and represents a $4f$ configuration close to the ground state. Also shown in Fig. 1(b) (long-dashed curve) is the much more bulk-sensitive $3d \rightarrow 4f$ resonant PE spectrum of $CeRh_3$ at 300 K, taken at $h\nu=884$ eV, where peak B is essentially absent. This identifies peak B in the surface-sensitive $4d \rightarrow 4f$ resonant PE spectrum as a signature of the surface layer [16]. Since the detailed analysis of the Ce $3d$ PE spectra [Fig. 1(a)] shows the absence of a temperature dependence of the surface contribution, peak B in Fig. 1(b) can be used as a reference for the intensity of peak A.

Within the SI model, peak A results from the hybridization of $4f$ states with the valence band; increasing hybridization should therefore lead to an increase in the relative intensity of peak A. In contrast to this, we find that the relative intensity of peak A decreases upon lowering the temperature to 20 K, i.e., with increasing $4f$ hybridization (see above). These observations contradict the SI model, but they are not at variance with bandlike $4f$ states, where an increase of internal pressure at low temperatures is expected to lead to a broadening of the narrow $4f$ bands causing a damping of the Fermi-level peak.

A further contradiction to expectations based on the SI model is observed in the fine structure of the Fermi-level peak in the $4f$ PE spectrum of $CeRh_3$ shown in Fig. 2. Peak A is split by spin-orbit interaction into two components (A_1 and A_2), separated by about 280 meV. On the basis of the SI model, the intensity ratio A_1/A_2 is expected to rise with increasing $4f$ hybridization [6]. While this is clearly reflected in the high-resolution resonant PE spectra of γ-Ce and α-Ce metal, shown for comparison in Fig. 2, the data for the most strongly hybridized system, $CeRh_3$, do not follow this systematic trend. Note that the $4d \rightarrow 4f$ resonant PE spectra of Fig. 2 contain again both bulk and surface contributions, where—in the case of α-

Ce—the intensity of peak A_2 has been shown to be almost entirely due to the presence of a γ-like surface layer and is almost zero for the pure bulk spectrum [17]. Taking a contribution from the more γ-like surface layer on $CeRh_3$ into account—as inferred from $3d$ core-level PE—the bulk $4f$ PE spectrum will be almost flat, while the larger $4f$ hybridization in $CeRh_3$ should lead—within the SI model—to an even stronger enhancement of component A_1 [6]. We note that crystal-field effects cannot explain the $4f$ PE spectrum of cubic $CeRh_3$. Even in tetragonal $CeSi_2$, where crystal-field effects are expected to be far more dominant, only the shape of peak A_1 was found to be affected, but not the intensity ratio A_1/A_2 [6].

An even stronger discrepancy with the SI model is observed for the room-temperature BIS spectrum of $CeRh_3$ displayed in Fig. 3. The BIS spectra of γ-like Ce systems are characterized by an intense $4f^2$ final-state multiplet situated about 4 eV above E_F, while α-like Ce systems exhibit an additional $4f^1$ peak close to E_F [4,18]. In $CeRh_3$, this $4f^1$ peak is shifted to an energy of 1.4 ± 0.1 eV above E_F, higher than in any other Ce compound studied so far, and the $4f^2$ contribution is rather weak. Note that the position of the $4f^1$ peak in $CeRh_3$ is well known from the systematic BIS study of a series of intermetallic Ce compounds presented in Ref. [19]. Further structures at $\simeq 3.3$ and $\simeq 8.5$ eV are due to transitions into unoccupied d-band states as confirmed by our LDA calculations (see inset in Fig. 3). The solid curve in Fig. 3(a) shows an analysis of the BIS spectrum within the SI model (Ref. [14]), using the $4f^2$-multiplet calculation of Ref. [20] and the bulk parameters from the above analysis of the $3d$ core-level PE spectrum ($\epsilon_f^b = -0.92$ eV; $\Delta^b = 1.0$ eV; $U_{ff} = 6.0$ eV) [13]. The underlying valence-band shape was taken from our LDA calculation and a 10% contribution to the BIS spectrum from a γ-like surface layer was assumed. Obviously, the positions of the $4f^1$ and $4f^2$ signals as well as the ratio of their intensities are reproduced incorrectly. An acceptable fit could only be achieved by using $\epsilon_f^b = -0.4 \pm 0.4$ eV, $\Delta^b = 1.9 \pm 0.2$ eV, and $U_{ff} = 3.2 \pm 0.4$ eV, with Δ about twice as large as derived from the $3d$ core-level PE spectra, and the Coulomb correlation energy U_{ff} reduced by a factor of $\simeq 2$. Such large deviations in the model parameters derived from BIS and PE spectra demonstrate the lack of a consistent description within the SI model. The fact that the derived values of U_{ff} and Δ are of comparable magnitude indicates the possibility for electron hopping between f states and the valence band, in agreement with a band picture for these states.

We have therefore also analyzed the BIS spectrum of $CeRh_3$ on the basis of the single-particle density of states (DOS) resulting from our LDA calculation (see inset of Fig. 3). In this approach, the calculated DOS was fitted to the experimental BIS spectrum, taking the ratio of f and d PE cross sections, the Lorentzian lifetime width, as well as the intensities of the spectrum and of the integral background as adjustable parameters. Finite experimental resolution was simulated by an additional Gaussian broadening, and the remaining $4f^2$ signal was added in the form of a final-state multiplet. The results are displayed in Fig. 3(b). It is obvious that the single-particle DOS describes the experimental data remarkably well, in particular, the position and shape of the $4f^1$ peak. The $4f^2$ intensity, on the other hand, amounts to about 30% of the whole $4f$ spectral intensity. Taking the surface sensitivity of BIS into account, the contribution from the γ-like surface layer can account for only a 15% $4f^2$ intensity. The remaining $4f^2$ spectral intensity represents a signal from bulk $CeRh_3$, which is not contained in the single-particle DOS. We interpret this signal as a $4f^2$ two-electron satellite caused by the correlated nature of the $4f$-band electrons. In this respect, this $4f^2$ satellite in BIS is closely related to the well-known 6-eV two-hole satellite in the valence-band PE spectrum of Ni metal [8].

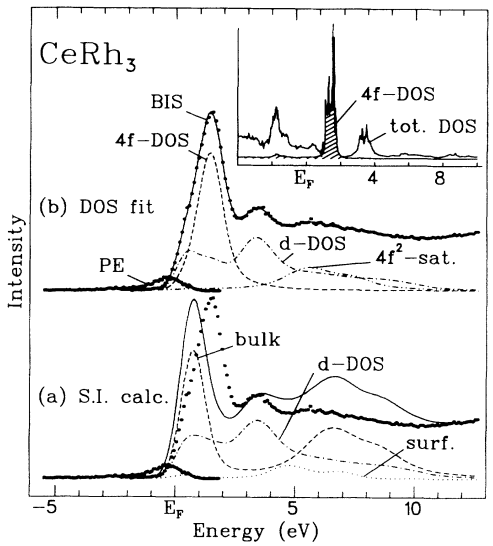

FIG. 3. Room-temperature BIS spectrum of $CeRh_3$ (solid points), measured with a total-system resolution of 0.6 eV (FWHM), and results of two different analyses (solid curves): (a) single-impurity model calculation with parameters derived from the $3d$ core-level PE spectrum; (b) fit using the calculated density of states displayed in the inset; for details see text. In addition, the weighted $4f$ PE spectrum, taken in $3d \rightarrow 4f$ resonance ($h\nu = 884$ eV) with a resolution of 0.7 eV (FWHM), is given (solid points); the two spectra overlap at E_F.

The present findings also demonstrate that the results of different high-energy spectroscopies cannot generally be compared in a direct way due to different degrees of localization of the final states. In core-level PE, the creation of a deep core hole will lead to increased localization. It is therefore not suitable for revealing band aspects of $4f$ electrons, since their effects on deep core-level PE spectra can always be described by a hybridization

parameter in a localized model. The additional electron in inverse PE causes the opposite effect. It is therefore not surprising that a $4f$ system at the borderline between localized and bandlike behavior can be described by the SI model in deep core-level PE, while a bandlike picture is apparently more appropriate in BIS; valence-band $4f$ PE is in between these two extremes. The difference between bandlike and localized character will show up most clearly in direct spectroscopies of the $4f$ density of states, as in $4f$ PE and particularly in BIS. While there is no doubt about the suitability of the SI model for interpreting spectroscopic data of weakly hybridized Ce systems, the present work clearly marks the limits of its applicability, where a description based on the bandlike ground-state is more favorable.

This work was supported by the Bundesminister für Forschung und Technologie, Project No. 05-5KEAXI/TP1, and the Swedish Natural Research Council.

[1] B. I. Min, H. F. J. Hansen, T. Oguchi, and A. J. Freeman, Phys. Rev. B **34**, 369 (1986); D. Glötzel, J. Phys. F **8**, L163 (1978); B. Johansson, Philos. Mag. **30**, 469 (1974).

[2] O. Eriksson, M. S. S. Brooks, and B. Johansson, Phys. Rev. B **41**, 7311 (1990).

[3] A. Yanase, J. Phys. F **16**, 1501 (1986).

[4] O. Gunnarsson and K. Schönhammer, Phys. Rev. B **28**, 4315 (1983).

[5] J. W. Allen, S. J. Oh, O. Gunnarsson, K. Schönhammer, M. B. Maple, M. S. Torikachvili, and I. Lindau, Adv. Phys. **35**, 275 (1986).

[6] F. Patthey, J.-M. Imer, W.-D. Schneider, H. Beck, Y. Baer, and B. Delley, Phys. Rev. B **42**, 8864 (1990).

[7] M. R. Norman, D. D. Koelling, A. J. Freeman, H. J. F. Hansen, B. I. Min, T. Oguchi, and Ling Ye, Phys. Rev. Lett. **53**, 1673 (1984).

[8] W. Nolting, W. Borgiel, V. Dose, and Th. Fauster, Phys. Rev. B **40**, 5015 (1989).

[9] J. C. Fuggle, F. U. Hillebrecht, Z. Zolnierek, R. Lässer, Ch. Freiburg, O. Gunnarsson, and K. Schönhammer, Phys. Rev. B **27**, 7330 (1983).

[10] O. K. Andersen, Phys. Rev. B **12**, 3060 (1975); H. L. Skriver, *The LMTO Method* (Springer-Verlag, Berlin, 1984).

[11] U. von Barth and L. Hedin, J. Phys. C **5**, 1629 (1972).

[12] O. Jepsen and O. K. Andersen, Solid State Commun. **9**, 1763 (1971).

[13] C. Laubschat, E. Weschke, C. Holtz, M. Domke, O. Strebel, and G. Kaindl, Phys. Rev. Lett. **65**, 1639 (1990).

[14] J.-M. Imer and E. Wouilloud, Z. Phys. B **66**, 153 (1987).

[15] L. C. Gupta, E. V. Sampathkumaran, R. Vijayaragharan, Varsha Prabhawalkar, P. D. Prabhawalkar, and B. D. Padalia, Phys. Rev. B **23**, 4283 (1981); N. Mårtensson, B. Reihl, W.-D. Schneider, V. Murgai, L. C. Gupta, and R. D. Parks, Phys. Rev. B **25**, 1446 (1982).

[16] C. Laubschat, E. Weschke, M. Domke, C. T. Simmons, and G. Kaindl, Surf. Sci. **269/270**, 605 (1992).

[17] E. Weschke, C. Laubschat, C. T. Simmons, M. Domke, O. Strebel, and G. Kaindl, Phys. Rev. B **44**, 8304 (1991).

[18] F. U. Hillebrecht, J. C. Fuggle, G. A. Sawatzky, M. Campagna, O. Gunnarsson, and K. Schönhammer, Phys. Rev. B **30**, 1777 (1984).

[19] W. Grentz, C. Laubschat, and G. Kaindl, Phys. Rev. B **36**, 8233 (1987).

[20] Y. Baer and W.-D. Schneider, in *Handbook of the Physics and Chemistry of Rare Earths,* edited by K. A. Gschneidner, Jr., L. Eyring, and S. Hüfner (North-Holland, Amsterdam, 1987), Vol. 10, p. 24.